5 Depth images of subduction processes

Both the migration of the unfiltered and the f-k filtered data sets were carried out because each of the resulting images highlights specific features. This is performed for Kirchhoff Prestack Depth Migration as well as for Fresnel Volume Migration. Several tests with additional preprocessing were accomplished including automatic gain control (AGC) to emphasise subsurface reflections rather than ocean bottom reflections or trace balancing (TB) to normalize the amplitudes within the shot gathers. Thereby, the aim was to find the combination which leads to the optimum images. Automatic gain control and trace balancing led to the best results, but the true amplitude character is then lost because both methods affect the recorded amplitudes. The intention of this work was not focused on dynamical estimates so that the preservation of true amplitudes was insignificant.

Within this chapter, the images resulting from Kirchhoff Prestack Depth Migration as well as additional features extracted with the help of Fresnel Volume Migration are presented. Each single shot gather was migrated separately. This enabled an additional stack of the absolute amplitude values of the resulting single shot depth sections. The obtained *absolute stack* images which show, in some cases, more details than the conventional stacked sections are also presented below.

5.1 Depth sections: Overview

Before detailed images are presented, the complete depth sections of both profiles are briefly illustrated and discussed to give an overview and a first impression of the main features along line SO104-07 as well as line SO104-13. Also a first insight is provided into the differences between Kirchhoff images and Fresnel Volume Migration results, both computed with the IFM-model (Figure 4.3). Complete sections resulting from migration with the corresponding wide-angle model are not shown as complete sections because they do not provide additional information in such a representation.

5.1.1 Results of line SO104-07

Figure 5.1 depicts the depth sections of profile SO104-07 where (a) represents the Kirchhoff Prestack Depth Migration and (b) the respective Fresnel image. The profile starts at about 72°W, crosses the trench at approximately 73 km and extends to the middle continental slope at 70°45′W to the east. These representations are not suitable to illustrate details but at the first glance several notable structures are observable.

A small seamount is located to the west of the trench, at about 15 km with a height up to 700 m. This seamount produces strong ocean bottom multiples disturbing the images in the subsurface. Due to their complex shape within the raw data they still appear even after Radon filtering. The roughness of the ocean bottom between the seamount and the trench at about 73 km indicates a possible horst and graben formation where the most pronounced structure is located between 55 km and 60 km along profile. Below the ocean bottom some features are vaguely visible on these images. Near the trench a first indicator for the subducted part of the Nazca plate can be found especially in the Fresnel result (Figure 5.1(b)). The seafloor of the lower and middle continental slope appears relatively smooth and the upper continental crust does not seem to contain considerable reflective structures. Comparing both images, a significant improvement is obtained after Fresnel Volume Migration. Except of the ocean bottom multiples below the seamount, almost all of the migration artifacts arising in the Kirchhoff result are suppressed.

5.1.2 Results of line SO104-13

The depth images obtained from line SO104-13 (Figure 5.2) clearly illustrate that the ocean bottom in this area is more rough compared to line SO104-07, i.e. possible horst and graben structures are more pronounced near the trench with flanks up to 1000 m high. Also the subducting Nazca plate is visible to about 80 km along profile. Underneath the lower and middle slope strong reflectivity occurs within the Kirchhoff images crossing the upper continental crust. Between 95 km and 110 km a normal fault system can be observed directly beneath the seafloor which is already known from further investigations (e.g. Hinz *et al.*, 1995; von Huene & Ranero, 2003). Again, the depth section obtained from Fresnel Volume Migration (Figure 5.2(b)) is improved compared to the Kirchhoff image (Figure 5.2(a)) mainly east of the trench where the latter exhibits strong migration smiles.

In the following sections detailed descriptions are given by means of enlarged zooms of the complete images.

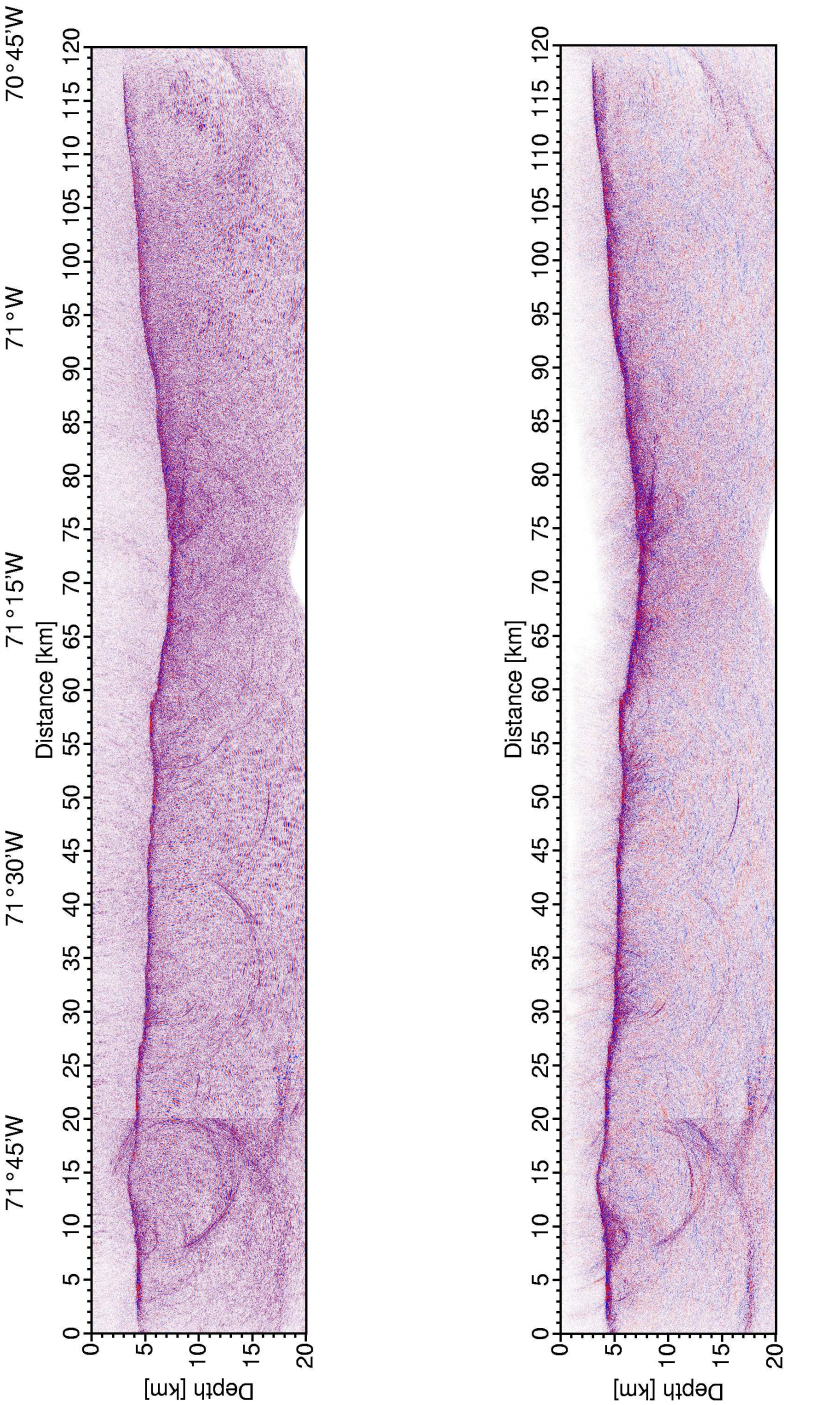

(a) Kirchhoff Prestack Depth Migration.

(b) Fresnel Volume Migration.

Figure 5.1: Depth images of the northern line SO104-07 at 21° S. (a) Kirchhoff Prestack Depth Migration (b) Fresnel Volume Migration. Both images were obtained using the IFM-model.

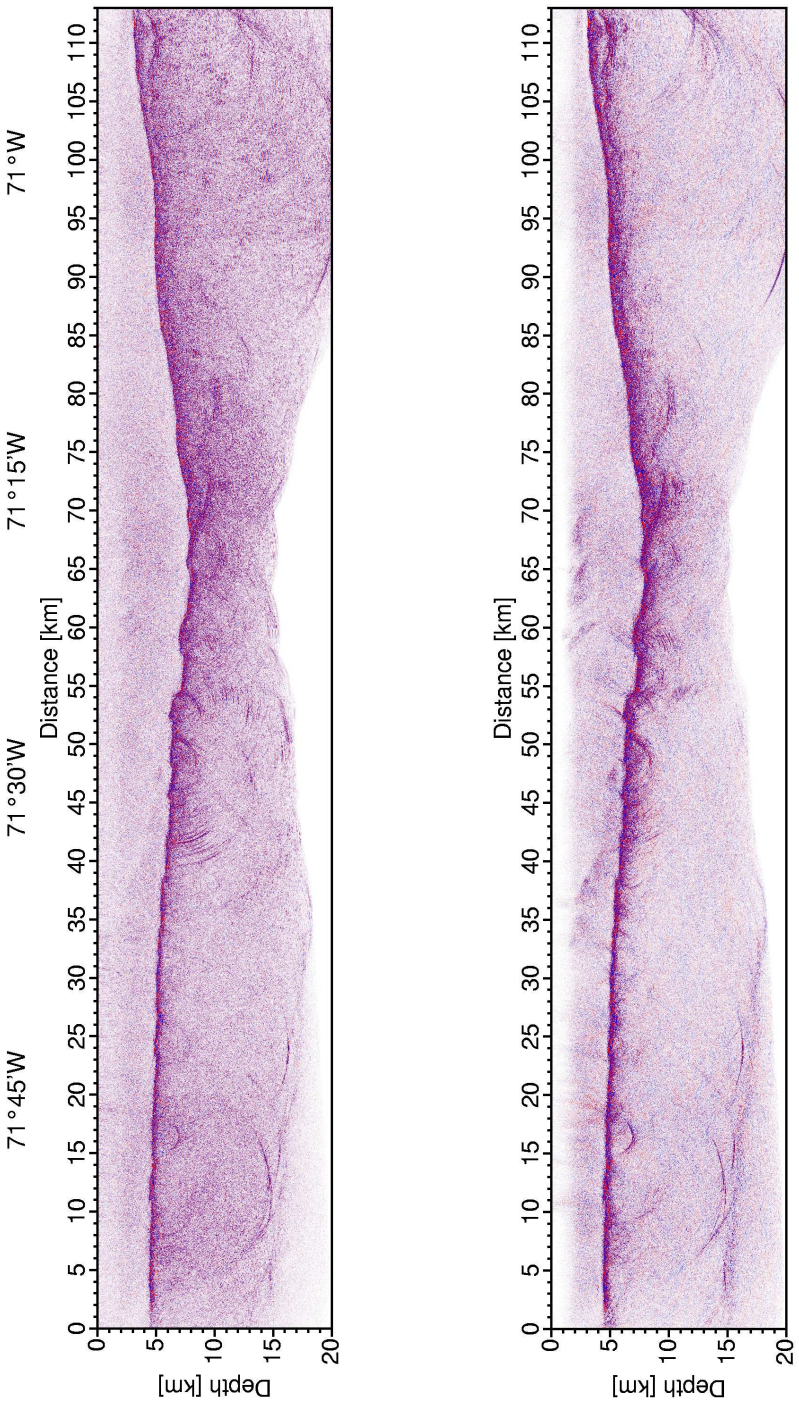

(a) Kirchhoff Prestack Depth Migration.

(b) Fresnel Volume Migration.

Figure 5.2: Depth images of the southern line SO104-13 at 23.25° *S. (a) Kirchhoff Prestack Depth Migration. (b) Fresnel Volume Migration. Both images were obtained using the IFM-model.*

5.2 Influence of the velocity models on the imaging results

To reveal the effect of working with different velocity models in the Kirchhoff Prestack Depth Migration results we focus on two sections, one for each profile (Figure 5.3). The upper plots exhibit a part from the beginning of line SO104-07 between 2 km and 7 km along profile (Figure 5.3(a) and (b)). In both illustrations, the ocean bottom is clearly imaged at the correct depth at approximately 4.2 km but the thickness of the sedimentary layers varies depending on which model is used.

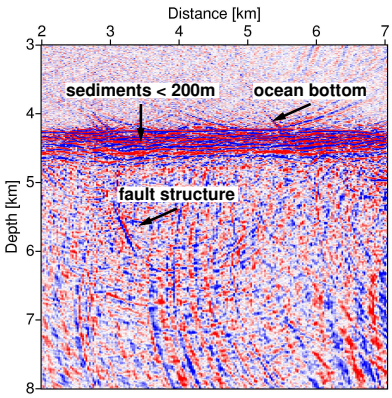

(a) *Depth image of a part of line SO104-07 obtained with the IFM-model.*

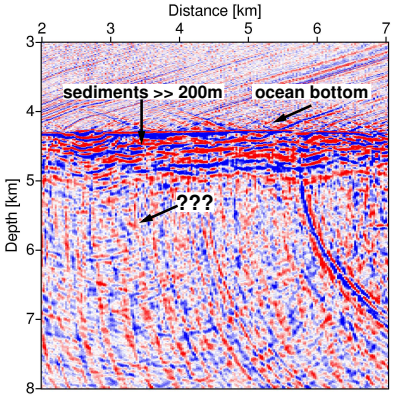

(b) *Same area as illustrated in (a) but computed with the wide-angle model.*

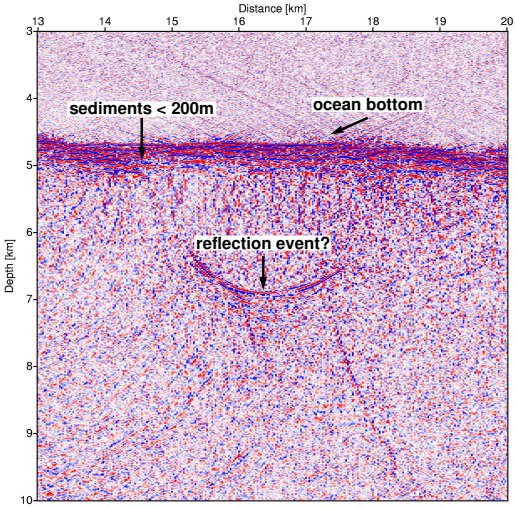

(c) *Part of the migration result of profile SO104-13 computed with the IFM-model.*

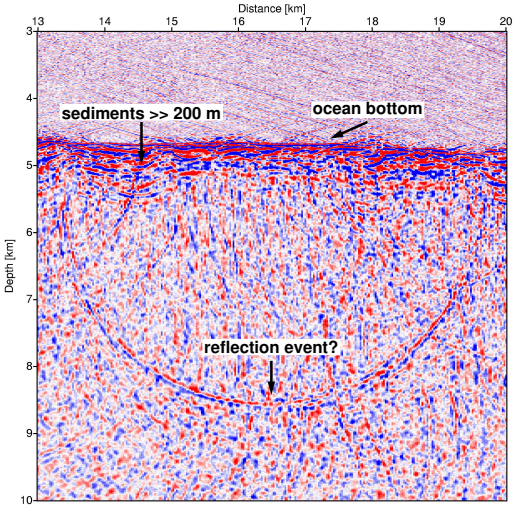

(d) *Same part as (c) migrated with the wide-angle model.*

Figure 5.3: Left hand side: Depth sections computed with the IFM-models. Right hand side: Corresponding images computed with wide-angle models. The upper images depict an area between 2 km and 7 km along profile SO104-07 and the lower images illustrate a part of line SO104-13 between 13 km and 20 km.

Working with the IFM-model, a maximum sediment thickness of less than 200 m is obtained which is equal to the expected value observed by several authors (e.g. Hinz *et al.*, 1995). In contrast, the sediments exceed a thickness of more than 300 - 400 m when the wide-angle velocity field is used. This effect is also visible in the images of line SO104-13 (Figure 5.3(c) and (d)). Here, a part between 13 km and 20 km is illustrated. At a depth range between 5 km and 6 km fault structure is visible in Figure 5.3(a). Due to the overall higher velocities within the wide-angle model, the isochrons get broader for a given travel time so that this fault structure vanishes in Figure 5.3(b)), i.e. it maps outside the regarded region. This fault has been observed on previous line drawings (Hinz *et al.*, 1995) at nearly the same location as seen on Figure 5.3(a). Just as the latter feature, the bowl-shaped reflection event observed in Figure 5.3(c) appears at greater depth when using the wide-angle model (Figure 5.3(d)) but produces a more pronounced migration smile. This could be an indicator for overmigration due to the use of too high velocities. Both, the overestimated sediment thickness and the strong migration smile from the reflector suggest that the P-wave velocities of the first one to two kilometers below the seafloor are too high within the model obtained from wide-angle measurements.

From a depth of about 6 km down to 14 km, a converse behaviour can be observed as illustrated in Figure 5.4. A weak reflection event emerges at approximately 6.5 km depth in Figure 5.4(a) superimposed by migration smiles whose origin might be the tectonic structure at the seafloor at 11 km along profile. In contrast, the image obtained with the wide-angle model (Figure 5.4(b)) shows this reflection at a depth of about 10 km - 11 km. This depth range corresponds to the expected Moho depth (approx. 7 km below seafloor, cf. Figures 5.23). Furthermore, the migration smiles

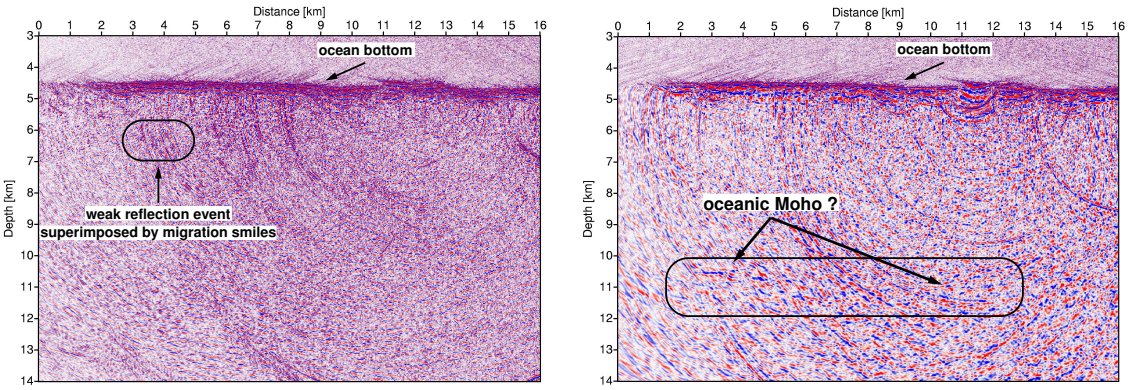

(a) Depth section of the first few kilometers of line SO104-13.

(b) The same section but migrated with the wide-angle model.

Figure 5.4: Two different depth sections of the same area along line SO104-13. (a) Image computed with the IFM-model. (b) Image computed with the wide-angle model.

are more dispersed within this image. These observations suggest that the use of the wide-angle model might be more reliable to image structures at greater depths.

The resulting depth images as discussed above indicate that the most reliable model might be a mixture of both initial models. Thus, the near surface part of the IFM-models are proposed to be closer to reality but for deeper regions the wide-angle velocities should be used. The main problem arising from the observations is the localisation of the seismic boundary (or transition zone) below the sediments where the P-wave velocities increase from low to high values. Flüh *et al.* (1997) observed an approximately 1 km thick layer with lower velocities in the uppermost part of the oceanic crust at 21°S compared to that of the wide-angle model (Figure 4.7(a)). At 23.25°, this layer is not as thick but it reaches depths of about 800m (Hinz *et al.*, 1995). Hence, the results are presented with respect to the regarded depth range in the following.

5.3 Migration results from line SO104-07

5.3.1 The ocean bottom and near-surface structures west of the trench

Starting from the origin of line SO104-07 (at about 72°W; cf. Figure 5.1), the most impressive structures which are not obvious in the overview plots are highlighted in the following. For a better orientation a scale of the complete profile can be found on top of each figure. Thereby, the green arrows mark the beginning and the red arrows depict the end of each illustrated enlargement with respect to the complete profile.

Underneath the ocean bottom to the west of the seamount between 6 km and 11 km along profile several reflection events indicate a highly fractured oceanic crust (Figure 5.5). The faults visible in the Kirchhoff image (surrounded by black ellipses in Figure 5.5(a)) seem to be more or less randomly oriented. The absolute stack of the Kirchhoff prestack depth migrated single shots (Figure 5.5(b)) slightly highlights these features. In the image obtained from Fresnel Volume Migration (Figure 5.5(c)) these features are clearly identified as fault structures. Thus, the Fresnel image enables a better interpretation (Figure 5.5(d)). Due to the straight-lined shape of the reflection events, they can not be interpreted as migration smiles.

The seamount itself contains no intra-crustal reflectivity, i.e. there are, at least, no features which can be resolved with the help of Kirchhoff Prestack Depth Migration. Also the Fresnel images of the seamount reveal only one or two additional small scaled features similar to that discussed above.